Kinetic Study of Tungsten Atoms (a $^7S_3$ and a ^5D_J) in the Presence of C_2H_4 and NH_3 at Room Temperature

Yo-ichi Ishikawa* and **Yoshitaka Matsumoto**

Department of Chemistry and Materials Technology, Kyoto Institute of Technology,
Matsugasaki, Sakyo-ku, Kyoto 606-8585

(Received November 18, 2002)

The gas-phase reactivity of W (a $^7S_3$ and a ^5D_J) with C_2H_4 and NH_3 at room temperature was investigated using a time-resolved laser induced fluorescence (LIF) spectroscopy. Tungsten atoms were produced by a 266-nm multiphoton decomposition (MPD) of $W(CO)_6$. The reactant pressure dependence of the *pseudo*-first-order depletion rates of W (a $^7S_3$) could allow an estimation of the *pseudo*-second-order depletion rate constant of W (a $^7S_3$), $(4.5 \pm 0.5) \times 10^{-10}$ cm^3 molecule^{-1} s^{-1} for C_2H_4 and $(0.73 \pm 0.10) \times 10^{-10}$ for NH_3 at 6.0-Torr total pressure with an Ar buffer. A simulation of the transient curves based on a modification of the observed apparent decay rate constants, involving nearby a ^5D_J states in the presence of C_2H_4 and NH_3, allowed us to separately estimate the contribution of the chemical quenching (W (a $^7S_3$) + R → product(s)) and the physical quenching (W (a $^7S_3$) + R → W (a $^5D_1$) + R) processes. In the case of C_2H_4, chemical quenching appeared to dominate over the physical quenching, while the physical quenching was the main depletion process in the case of NH_3. The large reactivity of the W (a $^7S_3$) state not only for C_2H_4, but also for NH_3, is discussed in terms of the relativistic effects.

Many transition-metal atoms have a number of nearby states derived from the electronic configurations of d^{n-2} s^2 and d^{n-1} s^1, which give a chance to investigate how the electronic configuration affects the reactivity other than the energy. The gas-phase transition-metal chemistry has so far provided fundamental information for metal-ligand interactions.[1–3] Those experimental results would be useful for understanding the catalytic processes on the active sites of transition-metal surfaces and also for developing theoretical calculations involving a spin-orbit interaction or a configuration interaction, and so on.[4,5]

In the gas-phase reactions of W (a ^5D_J and a $^7S_3$) with some oxidants, the a $^7S_3$ ($5d^5$ $6s^1$) state reacts more efficiently with O_2, NO, N_2O, and SO_2 than the a ^5D_J ($5d^4$ $6s^2$) states,[6,7] suggesting that the electron configuration plays the dominant role in the kinetic behavior of gas-phase tungsten. All of these oxidation reactions are reported to be bimolecular, where the common product is thought to be WO, owing to the independence of the reaction rates with respect to the total pressure. The major depletion process for the a $^5D_1$, a $^5D_0$ and a $^7S_3$ states was reported to be chemical quenching, though the contribution of physical quenching could not be excluded completely for the a $^5D_2$, a $^5D_3$, and a $^5D_4$ states. Because the quenching rate constants of the a ^5D_J states were found to be characteristically *J*-dependent for these oxidants, except for SO_2, the oxidation mechanism has been thought to be direct oxygen atom abstraction, but not the electron transfer mechanism.[8] The reactivity of W atoms for other reactants, except for these oxidants, have not been reported so far.

Relativistic effects may become conspicuous in chemical reactions involving heavy elements, such as the third transition metals.[9,10] The relativistic contraction and stabilization of the s shells, from the inner up to valence shell, and the relativistic expansion and destabilization of the d shell can be expected to have a certain effect on the chemical and physical interactions of the transition-metal elements with the reactants. An anomalous gas-phase chemical tendency of Au_2 for CO, NH_3, and C_2H_4, which could not be extrapolated from the trends in the reactivity from Cu_2 to Ag_2, was interpreted in terms of relativistic effects.[11] The large reactivity of W_2 (X) with C_2H_4 and NH_3, compared with Cr_2 (X) and Mo_2 (X), was also thought to have originated from relativistic effects.[12] W (a $^7S_3$) atoms having naked 5d and 6s electrons would give a chance to study the relativistic effects in chemical reactions by a comparison of Cr (a $^7S_3$) and Mo (a $^7S_3$) atoms with the same electron configuration.

In this study, we measured the transient behavior of the low-lying states of a tungsten atom W (a ^5D_J and a $^7S_3$) upon an interaction with C_2H_4 as a typical π-acceptor, and NH_3 as a typical σ-donor in order to understand the relation between the electronic structure and the reaction mechanism. A low-lying energy level diagram of tungsten atom is shown in Fig. 1.[13] The a $^5D_0$ state with the d^4 s^2 configuration is the ground state, and the other a ^5D_J states ($1 \le J \le 4$) locate in an energy region lower than 6219 cm^{-1}. The a $^7S_3$ state with a different electron configuration of d^5 s^1 has only 2951 cm^{-1} more energy than the ground state. However, in such a crowded system, the transient behavior of each state must be affected by the physical quenching of nearby states as well as by the chemical quenching, especially in an experimental system where the multiphoton decomposition of metal carbonyl by focused laser light is used for the pulse production of transition atoms. We have tried to discriminate the two processes, chemical and physical quenching, by calculation trials of all the

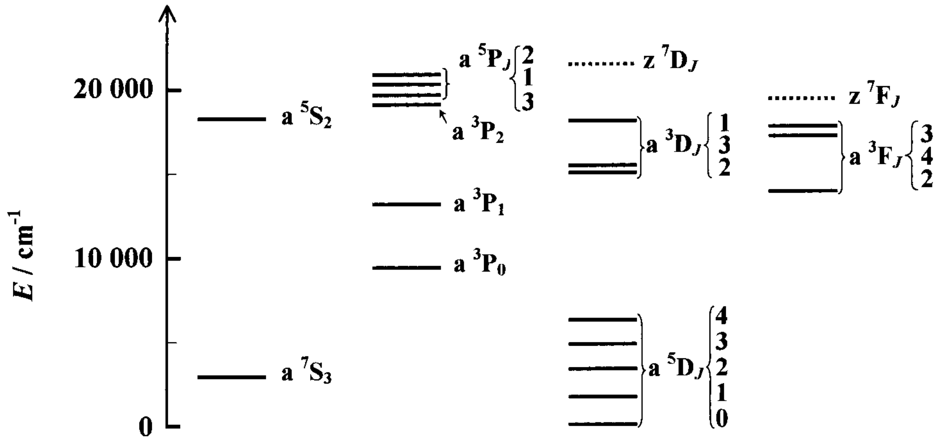

Fig. 1. Energy level diagram of W atom below 8000 cm^{-1}.

Table 1. Excitation and Monitoring Transitions Used in LIF Spectroscopy

Monitoring level	Excitation transition (λ/nm)	Monitoring transition (λ/nm)	Center wavelength of monochromator (20 nm fwhm) (λ/nm)
a $^5D_4$	z $^7D_3$ ← a $^5D_4$ (500.76)	z $^7D_3$ → a $^7S_3$ (430.33)	430
a $^5D_3$	z $^5P_2$ ← a $^5D_3$ (407.11)	z $^5P_2$ → a $^5D_2$ (383.61)	383
a $^5D_2$	z $^5P_2$ ← a $^5D_2$ (383.61)	z $^5P_2$ → a $^5D_2$ (383.61)	383
a $^5D_1$	z $^5F_2$ ← a $^5D_1$ (384.73)	z $^5F_2$ → a $^5D_1$ (384.73)	384
a $^5D_0$	z $^5F_1$ ← a $^5D_0$ (384.86)	z $^5F_1$ → a $^5D_0$ (384.86)	384
a $^7S_3$	z $^7P_2$ ← a $^7S_3$ (429.58)	z $^7P_2$ → a $^7S_3$ (429.58)	430

transient figures of the related states (a ^5D_J and a $^7S_3$) with one consistent set of rate constants obtained from a modification of the apparent decay rates. In a laser vaporization/flow tube/LIF experiment developed by Lian et al., Mo (a $^7S_3$) atoms have been reported to react with C_2H_4, but not to react with NH_3.[14] Such a specific reactivity was discussed in terms of the extent for reduction of the electronic repulsive interaction as an early barrier. Another object of this study was to see whether the trend of reactivity can persist in W atoms of the same group Ⅵ concerning relativistic effects.

Experimental

The concentration of each low-lying electronic state of tungsten atom was pursued by using a time-resolved LIF technique in a mass-flow-controlled cell at room temperature. Our time-resolved LIF apparatus was very similar to a typical one.[15,16] A photolysis 266-nm light source was a pulsed Nd:YAG laser (Spectron SL 803, $\lambda = 266$ nm). The laser beam, after passing through a Teflon iris (6 mm in diameter), was focused onto the center of a reaction cell using a quartz lens ($f = 15$ cm). As a source of resonance light for LIF, a Nd:YAG laser (Spectra-Physics GCR290-10) pumped dye laser (Lumonics HD-500) with a dye of Stilbene 420 (2×10^{-4} M in CH_3OH) was used with a 10 Hz repetition rate synchronized with the photolysis light by a digital delay generator (SRS DG535). The electronic transition used to monitor each state and the associated wavelength of the monochromator for fluorescence observation are given in Table 1. The fluorescence was detected by a photomultiplier (Hamamatsu R-928) set behind an exit slit of the monochromator (Spex Minimate; $f = 20$ cm, reciprocal dispersion = 4 nm/mm), the output of which was subsequently sent to a digital oscilloscope (Tektronix TD320). The digital output was stored and analyzed by a PC. The typical average laser shots were 256 to obtain an LIF intensity corresponding to W atom concentration at each delay time. $W(CO)_6$ (Aldrich, 98%) was degassed by several freeze-thaw cycles at -10°C and used without further purification. A sample mixture of $W(CO)_6$ ($\lesssim$10 mTorr) and Ar as a carrier gas was allowed to flow slowly through a brass cell with two suprasil windows. The flow quantity of each gas was controlled by a calibrated mass-flow controller (STEC-400MARK2 or 3: full scale, 10 sccm; accuracy, $< \pm 0.2$ sccm) prior to admission to the reaction cell. The mass-flow controller was used as purchased without any further calibration. The total mass-flow rates were between 5–10 sccm, and the reactant (C_2H_4 and NH_3) flow rates were 0.02–1.0 sccm. The total pressure was kept constant at 6.0 Torr with an Ar buffer, which was monitored with a capacitance manometer (MKS 220BH: full scale, 10 Torr; accuracy, $< \pm 0.015$

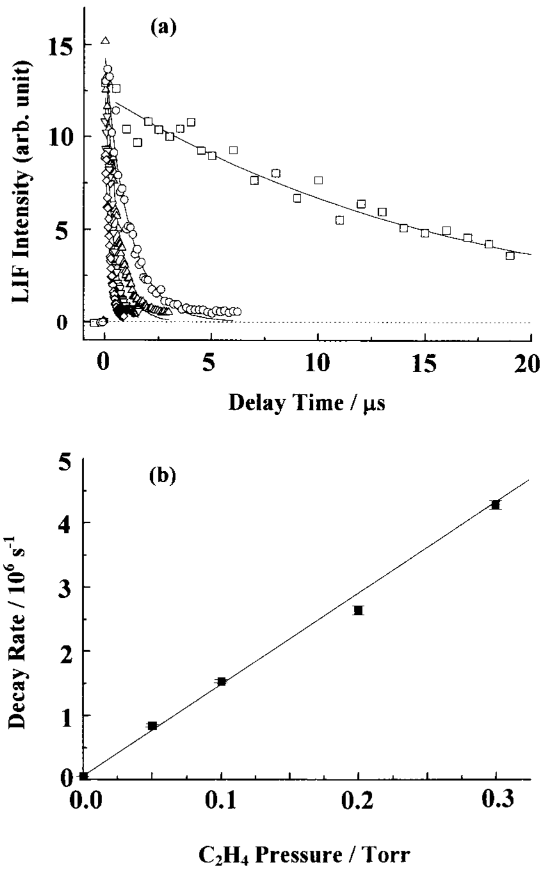

Fig. 2. (a) C_2H_4 addition effects on the transient LIF curves of W (a $^7S_3$) at 6.0-Torr total pressure with Ar buffer gas. C_2H_4 pressures are 0.0 (□), 0.05 (○), 0.1 (△), 0.2 (▽), and 0.3 Torr (◇). Each solid line is a single-exponential decay fit obtained with an appropriate decay rate constant. (b) Determination of the apparent second-order depletion rate constant. Solid line is a linear fit.

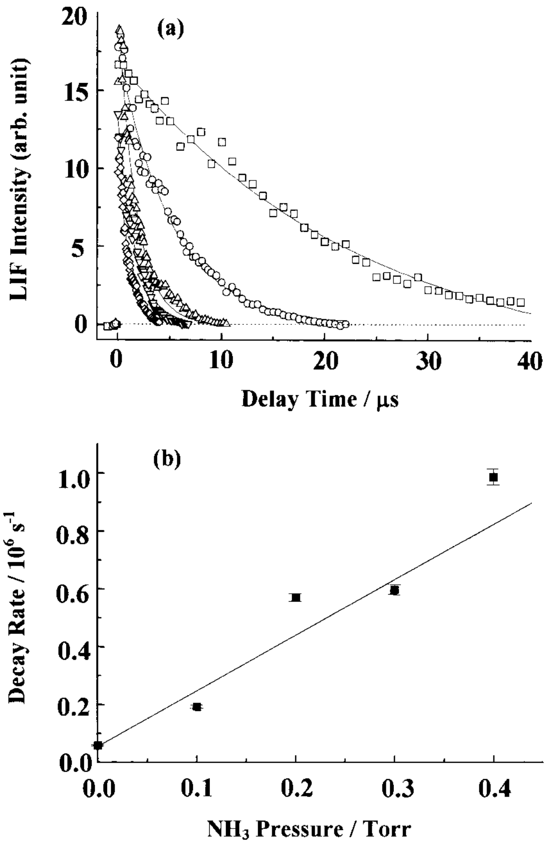

Fig. 3. (a) NH_3 addition effects on the transient LIF curves of W (a $^7S_3$) at 6.0-Torr total pressure with Ar buffer gas. NH_3 pressures are 0.0 (□), 0.1 (○), 0.2 (△), 0.3 (▽), and 0.4 Torr (◇). Each solid line is a single-exponential decay fit obtained with an appropriate decay rate constant. (b) Determination of the apparent second-order depletion rate constant. Solid line is a linear fit.

Torr) attached directly to the center of the flow cell.

Results

Typical depletion plots of W (a $^7S_3$) in the presence of C_2H_4 at 6.0-Torr total pressure using an Ar buffer are shown in Fig. 2(a), where approximate single-exponential decays were observed. The solid lines through data are single-exponential decay fits. These *pseudo*-first-order rates estimated from the single-exponential fitting increased proportionally with increasing the C_2H_4 pressure (Fig. 2(b)), giving an apparent second-order depletion rate constant of $(4.5 \pm 0.5) \times 10^{-10}$ cm^3 $molecule^{-1}$ s^{-1}. Similar plots obtained in the case of NH_3 addition are shown in Fig. 3. The apparent second-order depletion rate constant of $(0.73 \pm 0.10) \times 10^{-10}$ cm^3 $molecule^{-1}$ s^{-1} was estimated from the NH_3 pressure dependence of the *pseudo*-first order decay rates (Fig. 3(b)). Each error was one statistical deviation ($\pm\sigma$) in the linear fitting. W (a $^7S_3$, d^5 s^1) is more interactive with C_2H_4 than with NH_3 in a similar manner as Mo (a $^7S_3$, d^5 s^1).

Because a multiphoton decomposition (MPD) of $W(CO)_6$ was used for the pulse production of metal species in our experiment, many electronic states other than the a $^7S_3$ state were inevitably produced. The a $^7S_3$ state is metastable in W, differing from Cr and Mo, and the transient of this state must be affected by physical quenching from/to nearby states. Thus, the transient behaviors of some low-lying states of tungsten (a ^5D_J) in addition to the a $^7S_3$ state were also investigated as a function of the reactant pressure (C_2H_4 or NH_3) in order to distinguish between the chemical quenching and the physical quenching to nearby states.

Figures 4 and 5 show the addition effects of C_2H_4 and NH_3 on the transients of W (a ^5D_J) together with W (a $^7S_3$) at a total pressure of 6.0 Torr with an Ar buffer. The apparent depletion rate constants estimated from the additive concentration dependence of the decay rates are summarized in the third column of Tables 2 and 3. Each solid line in the figures is a calculated curve based on the assumption of an appropriate mechanism involving physical and chemical quenching processes, as mentioned below. Without any additives, except for Ar buffer (6.0 Torr) and a trace of $W(CO)_6$ ($\lesssim$10 mTorr) as precursor of W atoms, each electronic state (a ^5D_J and a $^7S_3$) shows a characteristic transient behavior, as shown by the open square symbols in each figure. The apparent growth in the a $^5D_4$, a $^5D_3$, a $^5D_1$ and a $^5D_0$ states indicates the occurrence of the physical quenching of the upper states correlating to these states, probably by Ar. The lack of growth in the a

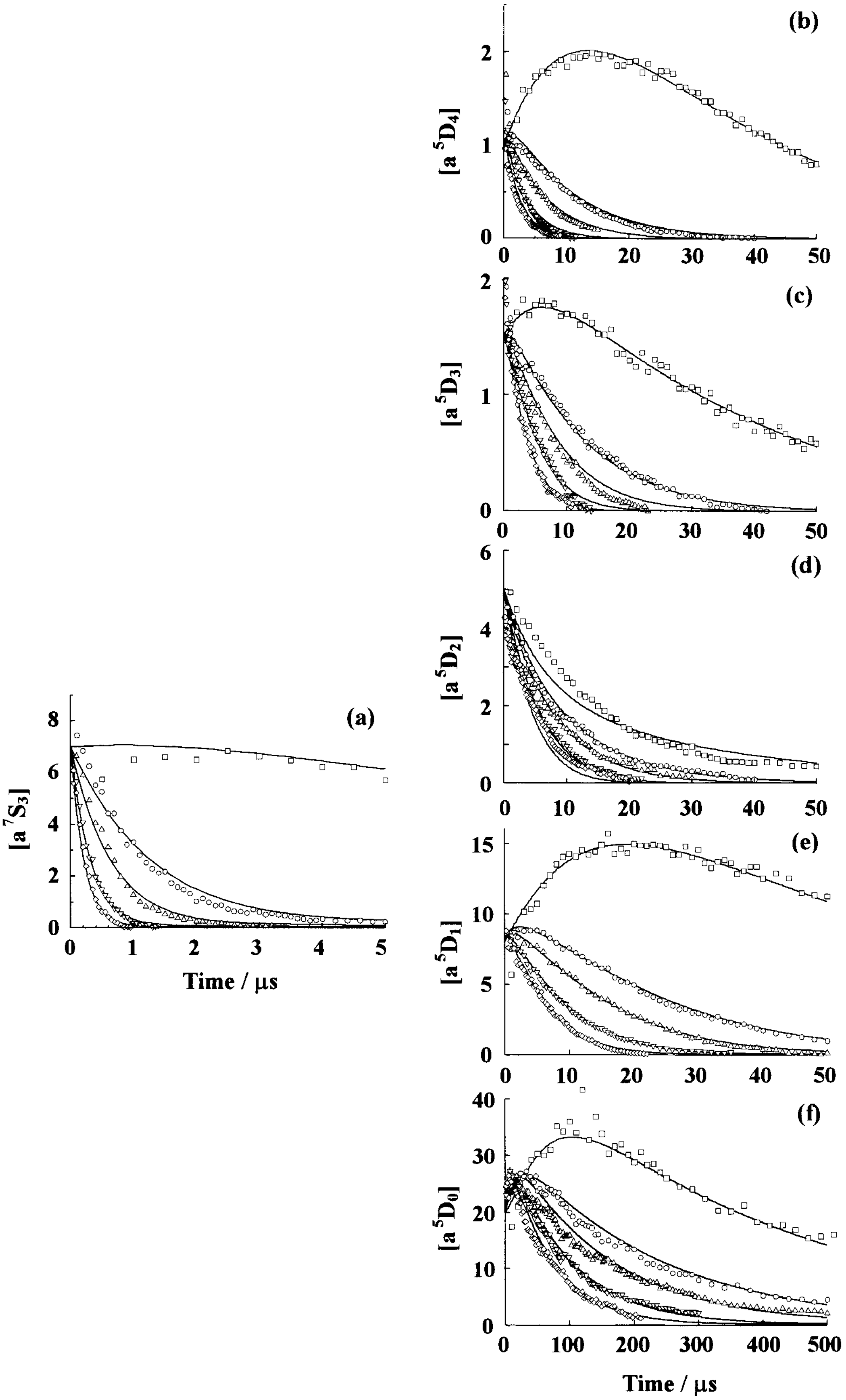

Fig. 4. C_2H_4 addition effects on the transient LIF curves of W (a $^7S_3$) (a) and W (a ^5D_J ; $J = 4$ (b), 3 (c), 2 (d), 1 (e), and 0 (f)) at 6.0-Torr total pressure with Ar buffer gas. C_2H_4 pressures are 0.0 (□), 0.05 (○), 0.1 (△), 0.2 (▽), and 0.3 Torr (◇). Each solid line is a calculation curve on the assumption of an appropriate mechanism involving physical and chemical quenching processes. See discussion in the text.

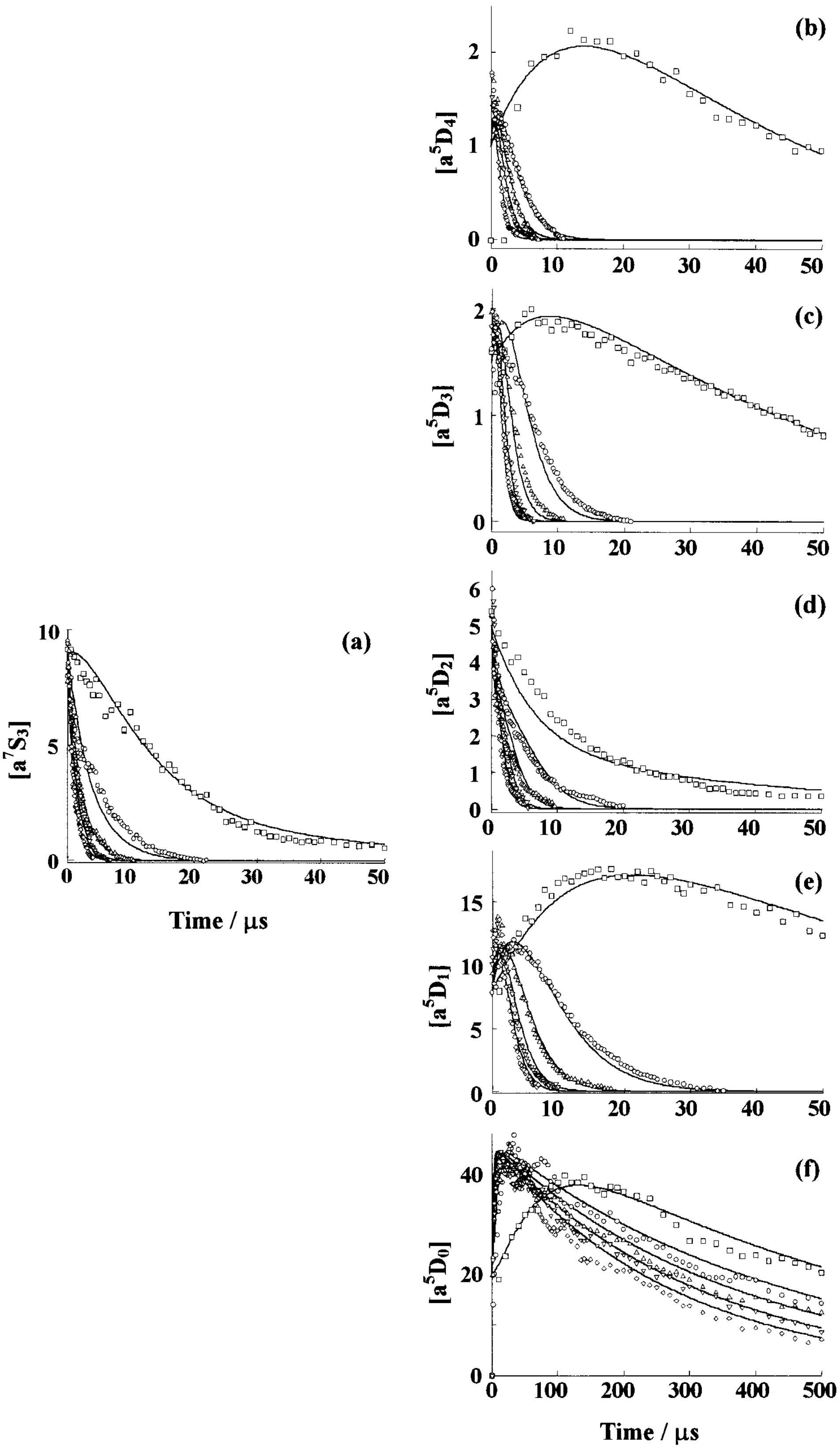

Fig. 5. (a) NH_3 addition effects on the transient LIF curves of W (a $^7S_3$) (a) and W (a ^5D_J ; $J = 4$ (b), 3 (c), 2 (d), 1 (e), and 0 (f)) at 6.0-Torr total pressure with Ar buffer gas. NH_3 pressures are 0.0 (□), 0.1 (○), 0.2 (△), 0.3 (▽), and 0.4 Torr (◇). Each solid line is a calculation curve on the assumption of an appropriate mechanism involving physical and chemical quenching processes. See discussion in the text.

Table 2. Second-Order Rate Constants ($k^{(2)}_{\text{apparent}}$, $k^{(2)}_{\text{physical}}$, and $k^{(2)}_{\text{chemical}}/10^{-10}$ cm^3 molecule^{-1} s^{-1}) of W (a ^5D_J and a $^7S_3$) with C_2H_4 at Room Temperature

State (R.P.)[a]	Level energy /cm^{-1}	$k^{(2)}_{\text{apparent}}$	$k^{(2)}_{\text{chemical}}$ (σ/Å^2)[b]	$k^{(2)}_{\text{physical}}$ (σ/Å^2)[b]
a $^5D_4$ (1.0)	6219.33	0.42 ± 0.04[c]	~0.013[d] (0.002)	0.40 (0.074)
a $^5D_3$ (1.5)	4830.00	0.28 ± 0.02	~0.013 (0.002)	0.35 (0.065)
a $^5D_2$ (5.0)	3325.53	0.11 ± 0.02	~0.013 (0.002)	~0.05 (→ a $^7S_3$) (0.009) 0.20 (→ a $^5D_1$) (0.037)
a $^7S_3$ (9.0)	2951.29	4.5 ± 0.5	5.2 (0.96)	~0.05 (→ a $^5D_2$) (0.009) 0.10 (→ a $^5D_1$) (0.018)
a $^5D_1$ (8.0)	1670.30	0.14 ± 0.01	~0.013 (0.002)	0.20 (0.037)
a $^5D_0$ (20.0)	0	0.013 ± 0.002	0.013 (0.002)	—

a) Presumed relative initial population for kinetic simulation. b) The absolute cross section σ ($= k/<v>$); $<v> = (8kT/\pi\mu)^{1/2} = 541$ m s^{-1}. c) One standard deviation of the linear fitting. d) A swung mark (~) means that the simulation is not sensitive to the value probably including ±200–300% error.

Table 3. Second-Order Rate Constants ($k^{(2)}_{\text{apparent}}$, $k^{(2)}_{\text{physical}}$, and $k^{(2)}_{\text{chemical}}/10^{-10}$ cm^3 molecule^{-1} s^{-1}) of W (a ^5D_J and a $^7S_3$) with NH_3 at Room Temperature

State (R.P.)[a]	Level energy /cm^{-1}	$k^{(2)}_{\text{apparent}}$	$k^{(2)}_{\text{chemical}}$ (σ/Å^2)[b]	$k^{(2)}_{\text{physical}}$ (σ/Å^2)[b]
a $^5D_4$ (1.0)	6219.33	0.84 ± 0.02[c]	~0.0015[d] (0.0002)	1.8 (0.27)
a $^5D_3$ (1.5)	4830.00	0.50 ± 0.03	~0.0015 (0.0002)	1.6 (0.24)
a $^5D_2$ (5.0)	3325.53	0.57 ± 0.05	~0.0015 (0.0002)	~0.30 (→ a $^7S_3$) (0.045) 0.90 (→ a $^5D_1$) (0.14)
a $^7S_3$ (9.0)	2951.29	0.73 ± 0.10	0.20 (0.03)	~0.20 (→ a $^5D_2$) (0.045) 0.70 (→ a $^5D_1$) (0.11)
a $^5D_1$ (8.0)	1670.30	0.37 ± 0.03	~0.0015 (0.0002)	0.52 (0.078)
a $^5D_0$ (20.0)	0	0.0015 ± 0.0004	0.0015 (0.0002)	—

a) Presumed relative initial population for kinetic simulation. b) The absolute cross section σ ($= k/<v>$); $<v> = (8kT/\pi\mu)^{1/2} = 663$ m s^{-1}. c) One standard deviation of the linear fitting. d) A swung mark (~) means that the simulation is not sensitive to the value probably including ±200–300% error.

$^5D_2$ state may be interpreted by a faster mixing with the a $^7S_3$ state, owing to the small energy gap of 370 cm^{-1}, or the larger initial concentration compared with the upper a $^5D_3$ and a $^5D_4$ states, so that the contribution of physical quenching to this state may be obscured at a glance. The concentration of the ground state of a $^5D_0$ increases until about 100 µs, and then decreases over a fairly long time (~ms). Upon the addition of reactants, the transient behaviors show that the a $^7S_3$ state is more interactive for C_2H_4 than any a ^5D_J states, and that the ground state (a $^5D_0$) is chemically less reactive for both reactants. The absence of a fast production of the a $^5D_1$ state synchronized with the fast decay of the a $^7S_3$ state by the addition of C_2H_4 suggests that the main depletion process of the a $^7S_3$ state is chemical quenching. Compared with the case of C_2H_4 (Fig. 4), there seem to be significant growths in the a $^5D_3$, a $^5D_1$, and a $^5D_0$ states by the addition of NH_3 in Fig. 5, suggesting that physical quenching is the main depletion process for the upper states of these states.

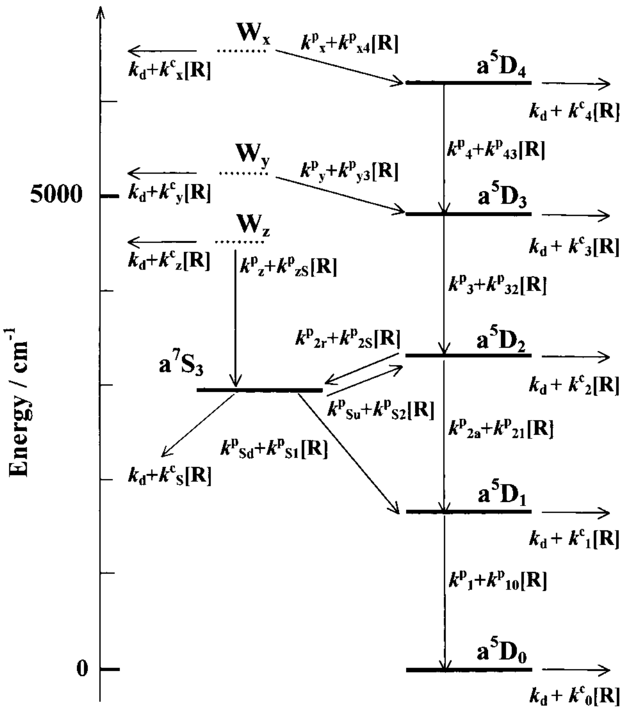

Fig. 6. An assumed quenching processes of W (a^7S_3, and a^5D_J) in the presence of C_2H_4 or NH_3 for the calculation of the transient concentrations of W (a^7S_3 and a^5D_J). In the kinetic schemes, k^c's are the chemical quenching constants and k^p's are the physical quenching constants.

Discussion

The addition of C_2H_4 or NH_3 on the transients of W (a ^5D_J) together with W (a $^7S_3$) at a total pressure of 6.0 Torr with an Ar buffer resulted in the following qualitative kinetic behaviors: a) W (a $^7S_3$) was more interactive with C_2H_4 than NH_3, while W (a ^5D_J) was less interactive with C_2H_4 than NH_3. b) The important quenching process for W (a $^7S_3$) by C_2H_4 seemed to be chemical, because fast production of the lower state (a $^5D_1$) corresponding to the decay of W (a $^7S_3$) was apparently not observed. c) The depression efficiency of the a $^7S_3$ state by NH_3 seemed to be comparable with those for the a ^5D_J states, except for the a $^5D_0$ state. d) There seemed to be some upper states which are physically quenched to the a $^5D_4$, a $^5D_3$, a $^5D_1$ and a $^5D_0$ states, mainly by Ar buffer.

Some numerical calculations were carried out in order to deduce *semi*-quantitative information about the kinetics of the a $^7S_3$ state and the a ^5D_J states with C_2H_4 and NH_3 from their transient data. The presumed kinetic mechanism used for the numerical calculation is shown in Fig. 6. In the kinetic schemes, $k^c{}_i$ is a *pseudo* second-order rate constant for chemical quenching of the *i*-state, and $k^p{}_{ij}$ is a physical quenching rate constant of the *i*-state to the *j*-state. Because the energy differences between two states of $\Delta J = 1$ in a ^5D_J multiplet were larger than 1390 cm^{-1}, which are fairly large compared to the thermal energy at room temperature ($\sim$200 cm^{-1}), any energy transfer from a lower state to an upper state in the a ^5D_J multiplet was ignored in the calculation, while the physical quenching between the a $^7S_3$ state and the a $^5D_2$ state was introduced to the calculation owing to its small energy gap of 374 cm^{-1}. At first, the transients of these states (a $^7S_3$ and a ^5D_J) observed under no reactant addition were simulated. This simulation fixed the relative initial concentrations of these six states and some rate constants unrelated to the reactant. The presumed initial concentration ratios are given in Tables 2 and 3, which are roughly similar to the Boltzmann distribution at 1800 K ($[^5D_4]:[^5D_3]:[^5D_2]:[^7S_3]:[^5D_1]:[^5D_0] = 1.0:2.4:5.7:10.7:12.7:16.1$) when the statistical weight $(2J+1)$ is taken into consideration. The difference in the initial concentrations between two systems of C_2H_4 and NH_3 might be due to the experimental scatter. Three states of W_x, W_y, and W_z had to be introduced into the reaction mechanism in order to simulate the rise behaviors of the corresponding three states: a $^5D_4$, a $^5D_3$, and a $^7S_3$. The possible candidates for these W_x, W_y, and W_z states are the upper states of a ^5D_J or a $^7S_3$, as shown in Fig. 1. The initial relative concentrations of the W_x, W_y, and W_z states were assumed to be 3.0, 1.5, and 2.0 when [a $^5D_4$] at $t = 0$ was set to 1.0. The residual parameters are the chemical and physical quenching rate constants of the reactant with W_x, W_y, W_z, a $^5D_4$, a $^5D_3$, a $^5D_2$, a $^7S_3$, a $^5D_1$, and a $^5D_0$ states, where the a $^5D_2$ and a $^7S_3$ states had two physical rate constants quenched to the a $^7S_3$ and a $^5D_1$ states and to the a $^5D_2$ and a $^5D_1$ states, respectively. The disappearance of W atoms due to an escape from an observation zone was postulated to have the same rate constant k_d $(= 2.5 \times 10^3$ s$^{-1})$ for all states. Because there is not any physical quenching process for the lowest state, a $^5D_0$, the slope of the decay rates vs reactant pressure plots was thought to give a chemical quenching rate constant, $k^c{}_0 = (1.3 \pm 0.2) \times 10^{-12}$ cm^3 s^{-1} for C_2H_4 and $k^c{}_0 = (1.5 \pm 0.4) \times 10^{-13}$ cm^3 s^{-1} for NH_3. In a simulation, it was assumed that these chemical quenching rate constants were adaptable for every a ^5D_J state. The physical quenching rate constants of the a ^5D_J states were estimated from the difference between the apparent total quenching rate constant and the chemical quenching rate constant, the values of which were used as the initial values in the trial calculation. Because the chemical quenching rate constants of the a ^5D_J states were fairly small compared to the apparent quenching process in both cases of C_2H_4 and NH_3, the alteration within one order in the chemical quenching rate constant did not affect these calculation curves significantly. It was therefore impossible to recognize the characteristically *J*-dependent of the chemical quenching rate constants of the a ^5D_J states, as observed for some oxidants.[6] The observed transient data without C_2H_4/NH_3, especially the three data sets in Figs. 4a, 4d, and 5d, show a substantial disagreement with the simulation results compared to the case with the reactant. This may suggest that there are some minor processes not included in our mechanism, such as the physical and chemical quenching by coordinatively unsaturated tungsten carbonyls or CO produced in photolysis. By the addition of the reactant, these minor processes may have less effect on the total reaction mechanism, owing to the appearance of the main processes with the reactant.

The rate constants estimated from the visual fittings for W (a ^5D_J and a $^7S_3$) are summarized in Table 2 (for C_2H_4) and Table 3 (for NH_3) together with the apparent second-order quenching rate constants. Some noticeable tendencies can be seen in their reactivity, though the resultant rate constants were not definitive because of the arbitrary kinetic model and of the arbitrary optimization of the fitting. The apparent second-order quenching rate constants of W (a $^7S_3$) with C_2H_4 and NH_3 of $(4.5 \pm 0.5) \times 10^{-10}$ and $(0.73 \pm 0.10) \times 10^{-10}$ cm^3 molecule^{-1} s^{-1}, estimated simply from the reactant pressure dependence of the *pseudo*-first-order depletion rates of W (a $^7S_3$), are slightly smaller than the sum of two rate constants for the physical and chemical processes. It seems to be reasonable that the state, which has an upper state with a tendency to be physically quenched, has a larger total quenching rate constant than the apparent depletion rate constant.

The a $^7S_3$ state is chemically more reactive with C_2H_4 than NH_3. Such a characteristic reactivity for the π-acceptor and σ-donor molecules has been observed in the ground state (a $^7S_3$) of the Mo atom, where the second-order rate constant for the Mo + C_2H_4 at 296 K was 2.3×10^{-13} cm^3 s^{-1} (at 7.8 Torr He), while that for the Mo + NH_3 was too small to be evaluated, $<5 \times 10^{-15}$ cm^3 s^{-1}.[14] Less reactivity of Cr (a $^7S_3$) for NH_3 and C_2H_4 has been observed at room temperature in the gas phase.[15,16] A significant reactivity of W (a $^7S_3$), even for a σ-donor (NH_3), contrary to the cases of Cr (a $^7S_3$) and Mo (a $^7S_3$), may be interpreted as indicating a larger polarizability of the tungsten atom caused by 6s/5d hybridization, though the reported values of the static average electric dipole polarizabilities for ground state these atoms (Cr; 11.6 (±2.9), Mo; 12.8 (±3.2), W; 11.1 (±2.8))[17] do not show such a tendency. A 6s-orbit contraction and stabilization as a result of relativistic effect may make this hybridization easier. However, some of the resultant collision complexes, W(NH_3), can be expected to be unstable and to dissociate spontaneously. This dissociation process would contribute to the physical quenching to the lower electronic state, while the stabilization process for a collision complex would contribute to the chemical quenching.

The a $^7S_3$ state ($5d^5$ $6s^1$) is chemically more reactive with C_2H_4 than any states of a ^5D_J ($5d^4$ $6s^2$) by a factor of 500 (Table 2). The bond formation of W (a $^7S_3$) with C_2H_4 can be interpreted by the Dewar-Chatt-Duncanson mechanism based on the analogy of the MO calculation of Mo (a $^7S_3$)–C_2H_4.[4,18,19] The chemical reaction of W (a $^7S_3$) with C_2H_4 could be treated as a second-order reaction in kinetic simulations, which may suggest that this addition pathway reaches a high-pressure limit, even at 6.0 Torr Ar buffer gas, and that the adduct complex W(C_2H_4)* has a rather long lifetime. In the s^1 configuration, the singly occupied d orbital of tungsten might overlap effectively with the vacant π^* orbital of C_2H_4 owing to the smaller electronic repulsion, weakening the C–C bond to form three-membered ring complex having some internal coordinates easy to flow into for the excess energy in the association coordinate. Such a long-lived M(alkene)* complex has been expected by a statistical unimolecular rate theory (RRKM theory), which assesses the plausibility of a saturated termolecular mechanism, even at 1 Torr He.[4] The reduction of the 6s electron repulsion for the π electron of C_2H_4 can be interpreted in terms of the formation of 6s/5d hybridization. The first step is a weak adsorption of the C_2H_4 on the W atom, which is connected with a spin flip from a septet to a quintet. This coordination may subsequently be assisted by a π-back donation, because of the relativistic extraction of the 5d orbital. The addition product of W(C_2H_4) is expected to have a bent structure with a triplet (or quintet) electronic state with a loose C···C bond, the interaction of which may be similar to the Cr (a $^7S_3$) + O_2.[5]

Table 4. Second Order Rate Constants $k^{(2)}$ for Chemical Quenching of W (a $^7S_3$, a ^5D_J) with Some Simple Molecules at ~300 K ($k^{(2)}/10^{-12}$ cm^3 molecule^{-1} s^{-1})

	O_2[a)]	NO[b)]	N_2O[b)]	SO_2[b)]	C_2H_4	NH_3
a $^5D_4$	1.8	7.1	1.5	36	~1.3	~0.15
a $^5D_3$	2.5	15	1.9	22		
a $^5D_2$	1.3	9.9	1.1	16		
a $^7S_3$	180	190	58	400	520	~20
a $^5D_1$	11	49	0.14	21	~1.3	~0.15
a $^5D_0$	1.6	28	0.003	6.0	1.3	0.15

a) Ref. 6. b) Ref. 7.

The second-order rate constants for the chemical quenching of W (a $^7S_3$) for C_2H_4 and NH_3 at room temperature are summarized in Table 4 together with the presumed constants of W (a ^5D_J). C_2H_4 is chemically reactive for the a $^7S_3$ ($5d^5$ $6s^1$) state as much as the oxidants,[6,7] and the electron configuration also plays an important role in the coordination reaction of C_2H_4 in the same manner as the oxidation reactions.

There seems to be slight difference in the efficiency of physical quenching between C_2H_4 and NH_3 for the a ^5D_J states, where NH_3 is observed to physically quench these states more effectively than C_2H_4. The degenerate deformation vibration frequency of NH_3 is 1627.5 cm^{-1} and the C=C stretching vibration frequency of C_2H_4 is 1623.3 cm^{-1}, which are approximately resonant with the energy gaps of the a ^5D_J manifold ($J = 0$ to $J = 1$, 1670.3 cm^{-1}; 1 to 2, 1655.2; 2 to 3, 1504.5; 3 to 4, 1389.3). The facts that the physical quenching efficiency of NH_3 is about a few times as large as that of C_2H_4, and that the physical quenching efficiency monotonously increases with increasing the level energy, are not consistent with the direct energy-transfer mechanism. These facts suggest that NH_3 is relatively easier to form a collision complex with a ^5D_J than C_2H_4 because the early barrier, probably for sd hybridization, may be overcome by the large dipole moment of NH_3. However, the resultant complex, W(NH_3), seems not to be stable at room temperature and to dissociate, where the a ^5D_J state may be physically quenched to the lower spin-orbit state. On the other hand, it is fairly difficult for C_2H_4 to overcome the early barrier because the electron density on C_2H_4 approaching the W atom is not high, resulting in the small quenching efficiency. The cross sections of intramultiplet mixing between the a ^5D_J states with $\Delta E \approx 1500$ cm^{-1} are on the order of 0.1 Å^2, which are smaller than those observed in the Cr (^7P_J) states with $\Delta E \approx 100$ cm^{-1} by two orders.[20]

Summary

The a $^7S_3$ state of the tungsten atom is chemically more reactive with C_2H_4 than with NH_3, though it does react chemically with NH_3 differing from the other group-6 elements

(Cr, Mo). Both reactions, W (a $^7S_3$) + C_2H_4 and W (a $^7S_3$) + NH_3, could be analyzed as being bimolecular, implying that even at a low total pressure of 6-Torr Ar the adduct complexes, $W(C_2H_4)^*$ or $W(NH_3)^*$, had a relatively long lifetime, enough for deactivation. The a $^7S_3$ state ($5d^5\,6s^1$) is chemically more reactive with C_2H_4 than any states of a ^5D_J ($5d^4\,6s^2$) by a factor of 500 (Table 2). The physical quenching appeared to dominate over the chemical quenching for W (a ^5D_J) in both cases of C_2H_4 and NH_3. The large interaction between W (a $^7S_3$) and W (a ^5D_J), not only with C_2H_4, but also with NH_3, is consistent with the relativistic contraction of the 6s shell and the relativistic expansion of the 5d shell.

We are grateful to Professor K. Honma (Himeji Institute of Technology) for useful comments on the kinetic interpretation. This work was supported by a Grant-in-Aid for Scientific Research (No. 11640508) from the Ministry of Education, Culture, Sports, Science and Technology.

References

1 Y. Wen, A. Yethirai, and J. C. Weisshaar, *J. Chem. Phys.*, **106**, 5509 (1997).

2 M. L. Campbell, *J. Phys. Chem. A*, **102**, 892 (1998).

3 K. Honma, *J. Phys. Chem. A*, **103**, 1809 (1999).

4 J. J. Carroll, K. L. Haug, J. C. Weisshaar, M. R. A. Blomberg, P. E. M. Siegbahn, and M. Svensson, *J. Phys. Chem.*, **99**, 13955 (1995).

5 A. Martinez, *J. Phys. Chem. A*, **102**, 1381 (1998).

6 M. L. Campbell and R. E. McClean, *J. Chem. Soc., Faraday Trans.*, **91**, 3787 (1995).

7 J. S. S. Harter, M. L. Campbell, and R. E. McClean, *Int. J. Chem. Kinet.*, **29**, 367 (1997).

8 K. Honma, M. Nakamura, D. E. Clemmer, and I. Koyano, *J. Phys. Chem.*, **98**, 13286 (1994).

9 K. S. Pitzer, *Acc. Chem. Res.*, **12**, 271 (1997).

10 P. Pyykkö, *Chem. Rev.*, **88**, 563 (1988).

11 L. Lian, P. A. Hackett, and D. M. Rayner, *J. Chem. Phys.*, **99**, 2583 (1993).

12 Y. Ishikawa and Y. Matsumoto, *Chem. Phys. Lett.*, **352**, 209 (2002).

13 "Atomic Energy Levels, Vol. Ⅲ," ed by C. E. Moore, NSRDS-NBS, 35, U.S. Government Printing Office, Washington D.C. (1971), p. 156.

14 L. Lian, S. A. Mitchell, and D. M. Rayner, *J. Phys. Chem.*, **98**, 11637 (1994).

15 J. M. Parnis, S. A. Mitchell, and P. A. Hackett, *J. Phys. Chem.*, **94**, 8152 (1990).

16 Y. Ishikawa, H. Ogawa, and T. Iwaki, *Bull. Chem. Soc. Jpn.*, **75**, 493 (2002).

17 "CRC Handbook of Chemistry and Physics, 70th Edition," ed by R. C. Weast, CRC Press, Inc., Boca Raton, Florida (1989–1990), E-72.

18 M. R. A. Blomberg, P. E. M. Siegbahn, and M. Svensson, *J. Phys. Chem.*, **96**, 9794 (1992).

19 J. J. Carroll, K. L. Haug, and J. C. Weisshaar, *J. Am. Chem. Soc.*, **115**, 6962 (1993).

20 J. M. Parson and T. Ishikawa, *J. Chem. Phys.*, **80**, 3137 (1984).